

Overview of Disturbance Reduction Requirements for LISA

Bonny L. Schumaker
Jet Propulsion Laboratory
California Institute of Technology
Pasadena, California 91109
E-mail: Bonny.L.Schumaker@jpl.nasa.gov

20 December 2001; revised 16 April 2002, 01 May 2002

Contents

1	Introduction	2
2	Requirements on LISA DRS	2
3	Control Model for DRS	4
4	Acceleration Disturbance sources	7
4.1	Spacecraft External Disturbances and Thruster Noise	7
4.2	Direct Proof-Mass Disturbances	8
4.3	Proof Mass - Spacecraft Coupling	13
5	Summary	15
6	References	20
7	Appendix A: Capacitive Sensor-induced Disturbances	21

1 Introduction

LISA must detect unequivocally an external force caused by passage of a gravitational wave. It infers the presence and characteristics of that force from interferometric observation of its effects on multiple optical paths of about five million kilometers in length, among three spacecraft trailing Earth in its heliocentric orbit. The interferometric phase measurements are hindered by their own noise sources, such as photon shot noise, inherent phase noise of the lasers and reference oscillators, and fluctuations in measured phase caused by pointing instabilities, wavefront curvature, and motion of optical components. Sensitivity to the gravitational-wave (GW) force is also hampered by competing effects of other fluctuating forces present, both external and internal to the spacecraft (SC). Minimization of these “spurious” (non-GW) accelerations is the task of the disturbance reduction system.

The disturbance reduction system comprises both sensing and control strategies, which work together to keep “proof masses” (PMs) in each of the three LISA spacecraft in as near a free-fall condition as possible. In the baseline design, there are two cube-shaped PMs within each of three identical spacecraft, separated from one another by about fifty centimeters and oriented at 60° , each facing one of the other distant spacecraft. Each PM must be in nearly perfect free-fall along the “sensitive axis” between it and the distant spacecraft to which it is pointed. The housing surrounding each PM, the telescope assembly to which each is optically connected, and the spacecraft that surrounds the pair of PMs must be controlled to maintain proper pointing and to minimize forces along the sensitive axis for each PM.

The overall design provides for a hierarchy of increasingly fine control over the minimum measurement bandwidth of 0.1 mHz to 1 Hz. Initially, the telescopes are pointed at the distant spacecraft via CCDs, quad-diodes, or other optical means. Small adjustments of the nominal 60° angle between the two telescopes can be made. Next, the SC are positioned to remain centered around the pair of PMs, in the plane of their sensitive axes, to within a few tens of nm/rt Hz. This is accomplished with a collection of FEOP thrusters, directed by the “drag-free” control loop, which receives information from position sensors around the PMs. These position sensors are key components in the disturbance reduction system. Their required sensitivity is derived and discussed briefly herein; their design and expected performance are subjects of vigorous ongoing studies by several research groups in Europe and the U.S. Finally, the PMs themselves are controlled along the non-sensitive axes to further center them in their housings. This direct control of the PMs must be accomplished in a way that produces negligible force along the sensitive axes in the measurement bandwidth, at least during science operations.

These control strategies are still in their study and development stages and are discussed in varying detail in several references. Considerable work remains to improve our understanding of error sources, of the performance, risks, and costs of baseline and alternative design options, and of various trade-offs. Development of an optical PM-SC displacement sensor as a backup or complement to LISA’s baseline capacitive sensors is a promising and logical activity. It also appears beneficial and cost-effective, some would argue even imperative, to develop one or more ground-based test facilities, such as a torsion-pendulum optimized for force measurements at LISA’s low frequencies, in order to assess different sensors and verify ability to achieve the required sensitivities. These and other tasks are discussed further elsewhere.

2 Requirements on LISA DRS

The LISA instrument is expected to be sensitive to a relative path-length change in the difference between two round-trip optical paths as small as $40 \text{ pm}/\sqrt{\text{Hz}}$ at frequencies around 3 mHz, where LISA’s sensitivity will be its best.[1] Below this frequency, LISA’s sensitivity becomes dominated by fluctuating acceleration disturbances to the PM which cause path-length errors that increase primarily as the inverse square of frequency ($1/\nu^2$). Above about 15 mHz, sensitivity decreases because the corresponding wavelengths of the gravitational waves are no longer large compared with the interferometer arm lengths of $5 \times 10^9 \text{ m}$. Photodetector shot noise and other errors specific to the optical phase measurements dominate at around 3 mHz. The portion of the (amplitude) noise spectral density for each PM position that comes from photodetector shot noise is about $10 \text{ pm}/\sqrt{\text{Hz}}$ across the entire measurement band of interest (assuming 30-cm telescope apertures, 1-W Nd:YAG lasers at wavelength 1.064 micron, and 30% overall optical efficiency). The purpose of the disturbance reduction system is to limit spurious acceleration disturbances in the frequency regime below 3 mHz, where they are the dominant error contribution to the overall measurement. The design goal

is a maximum total spurious (non-GW) acceleration disturbance of $3 \times 10^{-15} \text{ m/s}^2\sqrt{\text{Hz}}$ down to frequencies at least as low as 0.1 mHz.[1] This corresponds to force disturbances of $4 \times 10^{-15} \text{ N}/\sqrt{\text{Hz}}$ on the nominal 1.3-kg PM, and would result in contributions to PM position error (for each PM) on the order of 10 pm/ $\sqrt{\text{Hz}}$ at 3.0 mHz, 80 pm/ $\sqrt{\text{Hz}}$ at 1.0 mHz, and 8 nm/ $\sqrt{\text{Hz}}$ at 0.1 mHz. (See Table 1B.) Multiplying these numbers by four to account for the two round-trip optical paths gives the previously noted requirement of 40 pm/ $\sqrt{\text{Hz}}$ at 3 mHz.

This goal imposes a variety of stringent requirements on the LISA disturbance reduction system (DRS) as well as the spacecraft design and orbit. Because the PM is gravitationally coupled to the surrounding SC and both gravitationally and electrostatically coupled to its housing, it suffers both from acceleration fluctuations experienced by the SC (solar radiation pressure fluctuations and thruster noise) and from measurement error in the PM-housing displacement sensor that directs the SC drag-free control loop. In addition, the PM suffers from many other so-called “direct” disturbances which are independent of the coupling between the PM and its housing or the SC. Examples of direct disturbances include time-varying differential thermal radiation pressure caused by temperature fluctuations across the PM housing, random impacts from residual gas molecules in the PM housing, and voltage fluctuations on electrodes surrounding the PM that may be used for sensing the PM position relative to its housing. Section 4 below gives estimates of these disturbances and the requirements that may result. For example, temperature differences across the PM housings may have to be stabilized to about $6 \times 10^{-5} \text{ K}/\sqrt{\text{Hz}}$, outgassing may have to be suppressed sufficiently to ensure a local pressure lower than 3×10^{-12} atmospheres ($3 \times 10^{-7} \text{ Pa}$), voltages may have to be controlled to about $10^{-5} \text{ V}/\sqrt{\text{Hz}}$, and the PMs may need to be discharged as often as twice per day to ensure that the net charge build-up does not exceed about 10^{-13} Coulombs. Some of these requirements will pose a significant technological challenge at frequencies much lower than 0.1 mHz. Fortunately, the majority of the GW science data of greatest current interest is obtainable at frequencies higher than 0.1 mHz with a LISA-like instrument.

The PM disturbances associated with a coupling to the SC or DRS arise, by definition, from fluctuations in the position of the free-falling PM relative to its housing and the rest of the spacecraft. The physical forces that fluctuate with this PM-SC “displacement” come from gravitational gradients and from gradients in the capacitances (and their derivatives) between the PM and surrounding electrodes. Since, to a good approximation, these forces scale linearly with this displacement, their combined effect can be characterized as a spring-like force with coupling constant $K \equiv \omega_0^2$. The spring is “soft” because it is small in magnitude and thus has a low characteristic frequency ω_0 , and “negative” if it does not act to restore the PM to some equilibrium position over the measurement band (*i.e.*, ω_0 can be imaginary). Although individually these coupling forces may be small in magnitude, considerable effort is required to make their sum small enough to meet LISA’s sensitivity goal. The largest contributor to the coupling is thought to be gravitational gradients (see Table 3). Capacitive sensors, which are the baseline concept for monitoring the separation between PM and housing, are thought to be capable of the required performance, although not without technology development beyond what is currently available. Unfortunately, however, their performance has not been verified, on the ground or in flight, to closer than three orders of magnitude short of what LISA requires of them. Ground testing is challenged by seismic noise, but successful verification may be achieved by using sensitive torsion pendulums, which have been used successfully in other high-precision measurements of force.[16] Both analysis and testing are needed in order to understand and control several subtle but significant noise sources in capacitive sensors, such as voltage fluctuations and the presence of appreciable contact potentials (“patch fields”). Optical displacement sensors have also been considered for PM-housing displacement sensing, at least along the sensitive measurement axes [1, 13].

As noted above, because of the PM-SC coupling, the PM suffers both from SC acceleration fluctuations and from measurement error in the displacement sensor. Laboratory work to date with capacitive sensors suggests that the coupling constant can be made smaller than $10^{-7}/\text{sec}^2$; indeed, the idealized analysis presented below suggests that, in principle, the combination of sensor contributions and gravitational gradients might be kept below $10^{-8}/\text{sec}^2$ for the total PM-SC coupling constant K (see Table 3). This in turn would permit the displacement sensor error “ X_{nr} ” to be as large as about 30 nm/ $\sqrt{\text{Hz}}$ and still keep this contribution an order of magnitude smaller than the goal for the total of all acceleration disturbances. The required gain “ u ” of the SC drag-free control loop is determined both by the overall coupling constant K and by the SC disturbances. The latter, which arise from fluctuations in solar radiation pressure and from noise associated with the thrusters, will contribute several times $10^{-10} \text{ m/s}^2\sqrt{\text{Hz}}$ at 1 mHz. Multiplication

by $K/\omega^2 u$ to give the net acceleration disturbance experienced by the PM from this effect would require a gain u on the order of 100 to keep this contribution an order of magnitude smaller than the goal for the total of all acceleration disturbances. Table 1 uses the ambitious value of $5.3 \times 10^{-9} /s^2$ calculated herein for the total coupling constant K and requires only that each contribution to the total PM acceleration disturbance be held to one-half of the total requirement of $3 \times 10^{-15} \text{ m/s}^2\sqrt{\text{Hz}}$, resulting in more relaxed values for the sensor sensitivity X_{nr} and the SC control-loop gain. (See Table 1D.)

3 Control Model for DRS

Figure 1 shows a heuristic control model based on one introduced in [2], which describes the forces affecting both PM and spacecraft and the SC drag-free control loop that keeps the SC (*i.e.*, PM housing) centered on the PM. While this model depicts only one PM and is otherwise also less sophisticated than those being developed elsewhere, it is nevertheless adequate here for grouping disturbance sources according to how they contribute to PM position fluctuations, and for assessing the effects of parameters such as displacement sensor sensitivity (“ X_{nr} ” for “readout noise”) and drag-free control-loop gain ($u \equiv STR$). The control loop on the left side of the figure is the “drag-free” loop that uses micro-Newton thrusters on the SC to minimize displacements (from the centered position) of the PM housing with respect to the PM, along the sensitive axis. When considering only the sensitive axis of measurement for this PM, the PM actuator control loop on the right side of the figure can be ignored, to a first approximation. Similarly, when considering only the non-sensitive axes, the SC control loop can be ignored. These simplifications ignore cross-coupling between the sensitive and non-sensitive axes, an effect which may prove an important ultimate limitation, particularly in the actual design where a single spacecraft is positioned around two PMs with non-parallel sensitive axes. Cross-coupling will need to be understood better for specific DRS designs. The simple model used here is useful for categorizing and characterizing the major disturbance sources. Section 4 below derives estimates for magnitudes and scaling laws for these major disturbance sources. Based on those, critical technology challenges are then identified and requirements inferred for such areas as sensor and actuator performance, control-loop gains, PM charge management, and magnetic, thermal, and other environmental factors.

Figure 1 depicts the pathways of contribution to fluctuations in PM position which ultimately feed into the interferometer and combine with the other path-length error sources. The diagram can be used to solve for non-zero signal amplitudes, but here it will be used to propagate zero-mean disturbance amplitudes. The linear loop equations will be solved for the displacement disturbance amplitudes X_p and X_s of the PM and SC in terms of the other disturbances present, and the final magnitude of the fluctuations in PM or SC position can be estimated as the root-sum-square (rss) of statistically independent disturbances. The quantity $X_{ps} \equiv X_p - X_s$ represents fluctuations in the relative displacement between the PM and its housing; that displacement is monitored by the displacement sensor, fed into the SC drag-free control loop, and driven to zero mean by that loop. Additive position-measurement noise from the readout sensor is denoted by X_{nr} . The combined position fluctuations $X_{nr} + X_{ps}$ become an acceleration disturbance $A_r \equiv R(X_{ps} + X_{nr})$ (a process denoted here by multiplication by a sensor transfer function R), which in turn feeds into the thrusters, along with the thrusters’ own additive acceleration noise N_t . At the output of the thrusters (*i.e.*, after multiplication by a dimensionless thruster transfer function T), these impose an acceleration disturbance A_t on the SC. Additional acceleration disturbances on the SC are A_{ns} , caused by external sources such as solar radiation pressure fluctuations, and A_{ps} , caused by the coupling forces between PM and SC. Analogous disturbances acting on the PM are noted on the right-hand side of the figure.

Because the disturbances are characterized in units of acceleration and not force, the transfer functions have a convenient symmetry. The PM-SC coupling $K \equiv \omega_0^2$ and sensor transfer function $R \equiv \omega_R^2$ convert displacements into accelerations and therefore have units of $1/\text{sec}^2$, or angular frequency squared; they need not, however, be assumed to be positive or real. The thruster and PM actuator transfer functions T and C are dimensionless. If one or the other of them is zero, as in the approximation used here that there is no PM control along the sensitive axis so $C \approx 0$, then the other (T , here) could be set to unity and its effects absorbed into R and N_t in numerical estimates. The functions S and P , which represent SC and PM dynamics and convert acceleration disturbances into position fluctuations, have units of sec^2 and can be viewed as equal and characterized by $1/\omega^2$, where $\omega \equiv 2\pi\nu$ and the frequency band for ν of greatest interest here is between about 10^{-4} Hz and 10^{-2} Hz .

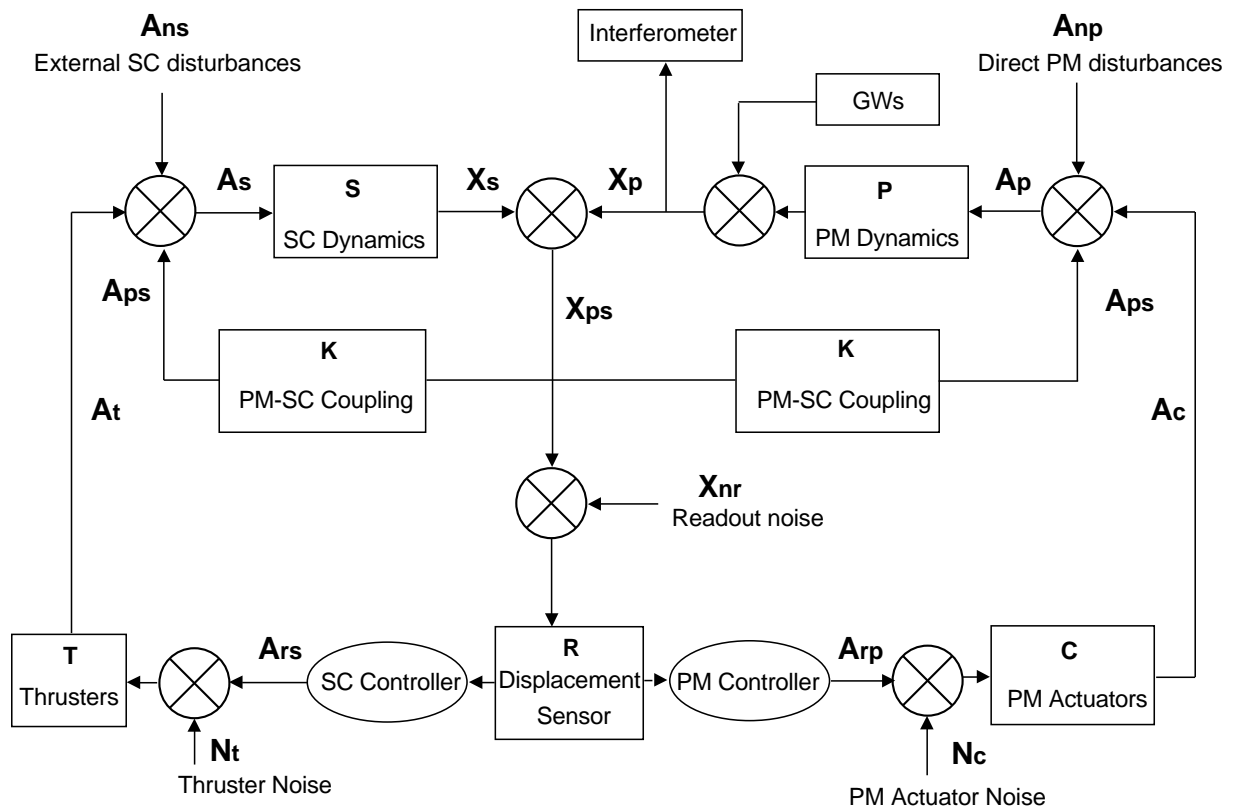


Figure 1: Control diagram for the LISA DRS system.

The loop equations are as follows. Sign conventions are consistent with those used for propagating non-zero-mean signal amplitudes; however, as noted above, contributions from the independent sources will be added quadratically to estimate the total magnitudes of the disturbances.

$$\begin{aligned} A_{rs}^{rp} &= \pm R(X_{ps} + X_{nr}); & A_{ps} &= KX_{ps} \\ A_c &= C(A_{rp} + N_c); & A_t &= T(A_{rs} + N_t); \\ A_s &= A_t + A_{ns} - (m_p/M_{sc})A_{ps}; & A_p &= A_c + A_{np} + A_{ps}; \end{aligned} \quad (1)$$

$$X_p \equiv PA_p; \quad X_s \equiv SA_s; \quad X_{ps} \equiv X_p - X_s, \quad (2)$$

where m_p and M_{sc} are the masses of the PM and SC, respectively. The resulting expressions for position fluctuations are:

$$\begin{aligned} X_p &= [1 - u - z - v - w]^{-1} [X_{nr}(z - zw + uv) + X_{np}(1 - u - w) + X_{ns}(-z - v)] \\ X_s &= [1 - u - z - v - w]^{-1} [X_{nr}(-u + uv - zw) + X_{np}(-u - w) + X_{ns}(1 - z - v)] \\ X_{ps} &= [1 - u - z - v - w]^{-1} [X_{nr}(z + u) + X_{np} - X_{ns}] \end{aligned} \quad (3)$$

where, for convenience, statistically independent quantities X_{np} and X_{ns} are defined as follows:

$$\begin{aligned} X_{np} &\equiv P(A_{np} + CN_c), \\ X_{ns} &\equiv S(A_{ns} + TN_t). \end{aligned} \quad (4)$$

The dimensionless quantities u , z , v , and w depend on the transfer functions:

$$\begin{aligned} u &\equiv STR = T\omega_r^2/\omega^2, \\ z &\equiv PCR = C\omega_r^2/\omega^2, \\ v &\equiv PK = \omega_0^2/\omega^2, \\ w &\equiv (m_p/M_{sc})SK = (m_p/M_{sc})v. \end{aligned} \quad (5)$$

The assumption $P = S = 1/\omega^2$ is, of course, a simplistic model for the actual frequency dependence of the transfer functions for these controllers. Note that the total acceleration disturbance A_p to the PM, for which the LISA goal is $3 \times 10^{-15} \text{ m}/(\text{s}^2\sqrt{\text{Hz}})$ down to frequencies as low as 0.1 mHz, is found by dividing the expression for X_p in equation (3) by the transfer function P .

In normal operation, the gain of the SC drag-free control loop, characterized by the dimensionless function $u = STR = T\omega_r^2/\omega^2$, is much larger than unity. Since this discussion is focusing on the SC drag-free control loop and control along the sensitive measurement axis, it can be assumed that disturbances from active PM control are negligible: $C \approx 0$, hence $z \approx 0$. Equations (3) then reduce to the following expressions for the fluctuations in PM and SC position:

$$\begin{aligned} X_p &= [1 - u - v - w]^{-1} [X_{nr}(uv) + X_{np}(1 - u - w) + X_{ns}(-v)] \\ &\approx X_{nr}(-v) + X_{np} + X_{ns}(v/u); \\ X_s &= [1 - u - v - w]^{-1} [X_{nr}(-u + uv) + X_{np}(-u - w) + X_{ns}(1 - v)] \\ &\approx X_{nr}(1 - v) + X_{np} + X_{ns}(-1 + v)/u; \\ X_{ps} &= [1 - u - v - w]^{-1} [X_{nr}(u) + X_{np} - X_{ns}] \\ &\approx -X_{nr} + X_{np}(-1/u) + X_{ns}(1/u). \end{aligned} \quad (6)$$

Multiplication by ω^2 gives the total acceleration disturbance to the PM:

$$\begin{aligned} A_p &= [1 - u - v - w]^{-1} [X_{nr}(uK) + A_{np}(1 - u - w) + (A_{ns} + TN_t)(-v)] \\ &\approx X_{nr}(-K) + A_{np} + (A_{ns} + TN_t)(K/\omega^2u). \end{aligned} \quad (7)$$

Similarly, the total acceleration disturbance to the SC is

$$\begin{aligned} A_s &= [1 - u - v - w]^{-1} [X_{nr} \omega^2 (-u + uv) + A_{np} (-u - w) + (A_{ns} + TN_t)(1 - v)] \\ &\approx X_{nr} \omega^2 (1 - K/\omega^2) + A_{np} + (A_{ns} + TN_t)(-\omega^2 + K)/\omega^2 u. \end{aligned} \quad (8)$$

For easy reference, expressions for the key quantities to be evaluated are repeated below, namely those for the PM acceleration disturbance $A_p \equiv \omega^2 X_p$, and the PM position fluctuations X_p (which feed into the interferometer measurement):

$$\begin{aligned} A_p &\approx X_{nr}(-K) + A_{np} + (A_{ns} + TN_t)(K/\omega^2 u); \\ X_p &\equiv A_p/\omega^2 \approx X_{nr}(-K/\omega^2) + X_{np} + X_{ns}(K/\omega^2 u). \end{aligned} \quad (9)$$

These expressions show explicitly the dependence on those quantities whose spectral natures and magnitudes figure critically in LISA’s ultimate performance and which will be evaluated below. These are: A_{np} , the total of all expected direct acceleration disturbances to the PM (excluding gravitational waves); $A_{ns} + TN_t$, the total of all external acceleration disturbances to the SC (solar radiation pressure and thruster fluctuations); K , the PM-SC coupling constant; u , the SC drag-free control-loop gain; and X_{nr} , the PM-SC displacement sensor readout sensitivity. To estimate the magnitude of the total acceleration disturbance experienced by the PM, one simply adds in quadrature the contributions of the terms in A_p [eq. (9)]. Multiplication by $P \equiv 1/\omega^2$ then gives the error in PM position, prior to addition of phase-measurement errors from the interferometer.

Keeping in mind that LISA must minimize the disturbance A_p to the PM, several observations can be made from these expressions. First, note from eq. (9) that “indirect” acceleration disturbances to the PM – those from readout sensor error ($\omega^2 X_{nr}$) and from SC external disturbances ($A_{ns} + TN_t$) – are suppressed relative to “direct” disturbances A_{np} both by the small dimensionless coupling constant $v \equiv K/\omega^2$ and the large SC drag-free control-loop gain u . Thus, it is imperative for LISA to have the dimensionless coupling K/ω^2 be much smaller than unity; at frequencies as low as 0.1 mHz, this will require that the “stiffness” K be smaller than $10^{-7}/s^2$.

Second, comparison between expressions (8) and (9) for the acceleration disturbances to the SC (A_s) and PM (A_p) shows that the “indirect” disturbances affect the SC to a greater extent than they do the PM, by a ratio of magnitude $|\omega^2/K - 1|$, which is greater than unity if the dimensionless coupling constant K/ω^2 is less than one-half (which will be satisfied for LISA frequencies down to 0.1 mHz or lower). For LISA, the DRS objective is to minimize the disturbance A_p to the PM, which requires that the coupling K/ω^2 be as small as possible. In contrast, if LISA functioned as an accelerometer, the DRS objective would be to minimize the total acceleration disturbance A_s to the SC, which would require that $K/\omega^2 \approx 1$ (resulting in $A_s \approx A_{np}$). Hence the LISA DRS sensors are described as “inertial” or “gravitational” rather than as accelerometers.

Third, note from eq. (6) that the required sensor sensitivity X_{nr} is comparable to the allowed fluctuation in PM-housing displacement X_{ps} . It will be shown below that both will need to be on the order of several tens of $\text{nm}/\sqrt{\text{Hz}}$ or smaller.

In the following sections, four independent quantities will be estimated: A_{ns} , the external SC acceleration disturbances, and TN_t , the acceleration fluctuations at the output of the thrusters (see Section 4.1); A_{np} , the direct disturbances to the PM that do not arise from coupling to the SC (see Section 4.2); and K , the coupling constant between PM and SC (see Section 4.3). Based on these estimates and the LISA goal for the total PM acceleration disturbance A_p , requirements are then inferred for the SC control-loop gain u and the displacement sensor readout sensitivity X_{nr} .

4 Acceleration Disturbance sources

4.1 Spacecraft External Disturbances and Thruster Noise

External disturbances to the SC come primarily from fluctuations inherent in the solar radiation flux, which produce corresponding fluctuations in the radiation pressure. Disturbances from random micrometeorite impacts and fluctuations in the solar wind are estimated to be several orders of magnitude less and hence

are ignored here. Estimates in the literature of the fractional fluctuations in solar irradiance W_0 differ by up to a factor of two.[14, 1] Recent estimates using VIRGO data [14] are consistent with about 0.13% at 1 mHz with a $\nu^{-1/3}$ frequency dependence (hence about 0.3% at 0.1 mHz):

$$\frac{\delta W_0}{W_0} \approx 1.3 \times 10^{-3} \left(\frac{1 \text{ mHz}}{\nu} \right)^{1/3} / \sqrt{\text{Hz}} . \quad (10)$$

Using a total irradiance of $W_0 \approx 1360 \text{ W/m}^2$, spacecraft area 4 m^2 and mass 300 kg gives

$$A_{ns, srp} = \frac{2A_{sc} \delta W_0}{M_{sc} c} = 1.6 \times 10^{-10} \text{ m/s}^2 \sqrt{\text{Hz}} \left(\frac{1 \text{ mHz}}{\nu} \right)^{1/3} \quad (11)$$

(about 3.4×10^{-10} at 0.1 mHz). The factor of two is for the pessimistic assumption of a perfectly reflecting surface. Equivalently, the force fluctuations on the SC from solar radiation pressure fluctuations are on the order of 50 nanoN/ $\sqrt{\text{Hz}}$ at 1 mHz. In a 1-mHz bandwidth, this would be about 2 nanoN, or about 12,500 times smaller than the dc solar radiation pressure force of about 20 microNewton for a perfectly absorbing solar panel.

Force fluctuations on the SC due to the thrusters have been estimated to be smaller than $10^{-7} \text{ N}/\sqrt{\text{Hz}}$ [15] corresponding to acceleration fluctuations TN_t on the order of $3 \times 10^{-10} \text{ m/s}^2 \sqrt{\text{Hz}}$, or roughly twice that from the solar radiation pressure fluctuations. (This value for thruster noise can be assumed to subsume the smaller contribution from digital-to-analog (D/A) quantization of the force adjustments. For a nominal 10-Hz update frequency and 12 bits, the quantization noise associated with a 100-microNewton thruster force is $10^{-4} \text{ N}/2^{12} \sqrt{120 \text{ Hz}} \approx 2 \times 10^{-9} \text{ N}/\sqrt{\text{Hz}}$.) The rss of these gives a total spacecraft external acceleration disturbance

$$A_{ns} + TN_t \approx 3.4 \times 10^{-10} \text{ m/s}^2 \sqrt{\text{Hz}} \quad \text{at 1 mHz} , \quad (12)$$

and about 35% larger than this at 0.1 mHz because of the $\nu^{-1/3}$ frequency dependence of the solar radiation pressure (see Table 1C).

Referring back to eq. (9), if the PM-SC coupling K can be made as small as $10^{-7}/\text{sec}^2$, then the contribution from SC disturbances to the total PM acceleration disturbance A_p will be $3.4 \times 10^{-17}/\omega^2 u \text{ m/s}^2 \sqrt{\text{Hz}}$. In order to ensure that this one contribution is at least an order of magnitude smaller than the total goal of $3 \times 10^{-15} \text{ m/s}^2 \sqrt{\text{Hz}}$, the SC control loop gain must satisfy $u \geq 0.11/\omega^2 \approx 2900$ at $\omega/2\pi = 1 \text{ mHz}$, and two orders of magnitude larger at 0.1 mHz. This is probably not unduly challenging. Table 1D shows a considerable relaxation of these values, by virtue of a 20-times smaller value for K and a requirement that the contribution be only a factor of two smaller than the total LISA goal for A_p .

It is interesting and entertaining to note that the dc solar radiation pressure force on the SC, at least 20 microNewton (up to a factor of two larger, to the extent that the SC is not perfectly absorbing), is equivalent to the weight on Earth of about 2 mg. This is comparable to about (1/25)the weight of a postage stamp, roughly the weight of a small binder-ring hole punched from a piece of paper![18] It is also comparable to the force that would be felt at the LISA SC from a quiet whisper at a distance of about 10 m. Note that the total disturbance limit allowed for the LISA PM, roughly 0.1 femtoNewton over a 1-mHz bandwidth, is equivalent to the weight on Earth of 0.01 picogram, or about 1% of the weight of a bacterium. This maximum allowed disturbance is comparable in magnitude to the force that would be felt at the LISA PM by a quiet whisper at a distance of about 70 km.

4.2 Direct Proof-Mass Disturbances

It is an involved task to estimate the contribution A_{np} of direct PM acceleration disturbances. There are at least fifteen estimable contributions (not counting gravitational waves). Four are magnetic effects; three are impact-type forces from cosmic rays, residual gas molecules, and laser photons; three arise from temperature fluctuations across the PM housing and the SC, which cause differential radiation pressure from residual gas and thermal radiation as well as time-varying gravitational disturbances *via* thermal distortion of nearby masses; and, finally, as many as five may arise from voltage and charge fluctuations on the PM and surrounding electrodes.

The PM is assumed to be a Pt-Au (10%-90%) alloy or equivalent with very low magnetic susceptibility $\chi_m \approx 10^{-6}$ and density $\rho \approx 2 \times 10^4 \text{ kg/m}^3$ (20 gm/cm³), consistent with a cube 4 cm on a side and mass

about 1.3 kg. The typical length scale for the SC is $r_{sc} \approx 1$ m. The average local magnetic field B_{sc} will arise primarily from the small permanent magnets used in conjunction with stabilization of the laser frequency. (These typically are glued to the laser crystal, effectively acting like a Faraday isolator to promote single-frequency operation.) An estimate for B_{sc} of 7×10^{-6} Tesla (T) was made in [8], corresponding to an average magnetic moment M_s of 1.5 A-m² at a distance of about $r_m \approx 35$ cm from the PM ($B_{sc} \approx 2\mu_0 M_s / 4\pi r_m^3$). The fluctuations from this field are unlikely to be larger than about $0.1\% / \sqrt{\text{Hz}}$ on time scales of interest. [8] The other possible source of fluctuations in the local SC magnetic field would be DC currents. These fields themselves are smaller, on the order of nano-Tesla, and the current fluctuations resulting from power dissipation are unlikely to cause significant magnetic field fluctuations.[9]

The average interplanetary magnetic field strength is about twenty times smaller, $B_{ip} \approx 3 \times 10^{-7}$ T, but it exhibits variations as large as 10% at 1 mHz, with roughly a $1/\nu$ frequency dependence: $|\delta B_{ip}| \approx 3 \times 10^{-8}$ T/ $\sqrt{\text{Hz}}$ (1 mHz/ ν). The total magnetic field is the vector sum $\vec{B} \equiv \vec{B}_{sc} + \vec{B}_{ip}$. In the presence of this magnetic field, a magnetic moment is induced in the PM, $\vec{M}_p \approx \chi V_p \vec{B} / 2\mu_0$, where V_p is the PM volume. The net force on the PM from this magnetic coupling has the form $\vec{b} \cdot \vec{M}_p$ multiplied by $3/r_m$ (equal to $4\pi r_m^2$ divided by the volume $4\pi r_m^3/3$). Thus, the PM experiences an acceleration proportional to the square of the total magnetic field, the two dominant terms of which are the square of the local field, B_{sc} , and the product $B_{sc} B_{ip}$ (the factor of two disappears on averaging the vector product). Fluctuations in these terms therefore scale as $2|\delta B_{sc}|$ and $|\delta B_{ip}|$, respectively. The corresponding PM acceleration disturbances are

$$A_1 \equiv \frac{1}{2} \chi_m \frac{1}{\rho\mu_0} 6 \frac{1}{\xi_m} 2B_{sc} \frac{1}{r_{sc}} |\delta B_{sc}|$$

$$\approx \frac{1}{\xi_m} 1.2 \times 10^{-17} \text{ m/s}^2 \sqrt{\text{Hz}} ; \quad (13)$$

$$A_2 \equiv \frac{1}{2} \chi_m \frac{1}{\rho\mu_0} 6 \frac{1}{\xi_m} B_{sc} \frac{1}{r_{sc}} |\delta B_{ip}|$$

$$\approx \frac{1}{\xi_m} 2.5 \times 10^{-17} \text{ m/s}^2 \sqrt{\text{Hz}} \left(\frac{1 \text{ mHz}}{\nu} \right) ; \quad (14)$$

where $\mu_0 = 1.26 \times 10^{-6}$ N/A² is the magnetic permeability of vacuum, and ξ_m is a scaling factor included to allow for possible suppression by magnetic shielding, which could be on the order of 10 to 20. The inverse frequency dependence of A_2 makes it a significant contributor at 0.1 mHz, which may make it desirable to reduce the mean SC magnetic field B_{sc} by a factor of five or so.[9]

Additional magnetic-related disturbance arises due to the Lorentz-force effect as the nonzero, fluctuating charge of the PM moves in orbit through the fluctuating interplanetary magnetic field. It is thought that the non-fluctuating (bias) contribution to this effect can be suppressed by more than an order of magnitude with electrostatic shielding, since in the rest frame of the PM the magnetic field appears as an electric field.[4] There will still be contributions to the acceleration fluctuations which remain to be analyzed for a given model of this type of shielding. The magnitude of the unsuppressed fluctuations can be calculated, however, and a shielding factor ξ_e will be included to allow for a possible suppression factor. The SC orbital velocity is

$$v = 1 \text{ AU} \cdot (2\pi/1 \text{ year}) \approx 3 \times 10^4 \text{ m/s} . \quad (15)$$

Estimates of the rate of charge buildup due to cosmic-ray impacts suggest an average rate equivalent to about 13 electrons per second, or $\dot{q} \leq 2 \times 10^{-18}$ Coulombs/sec.[1,3] At this rate, the charge could build up to 10^{-12} C in about one week, and to 10^{-13} C $\equiv q_0$ in about 14 hours. Assuming a Poisson distribution of impacts producing an average current spectral density $2e\dot{q}$ A²/Hz, where e is the electron charge, one infers an average charge fluctuation spectral density

$$\delta q \equiv \frac{(2e\dot{q})^{1/2}}{\omega} \text{ C}/\sqrt{\text{Hz}} \approx 1.3 \times 10^{-16} \left(\frac{1 \text{ mHz}}{\nu} \right) \text{ C}/\sqrt{\text{Hz}} . \quad (16)$$

The resulting acceleration disturbances to the PM are

$$A_3 \equiv \frac{1}{\xi_e} \frac{v}{m_p} |\delta q| B_{ip} \approx 10^{-19} \left(\frac{10}{\xi_e} \right) \left(\frac{1 \text{ mHz}}{\nu} \right) \text{ m/s}^2 \sqrt{\text{Hz}} ; \quad (17)$$

$$A_4 \equiv \frac{1}{\xi_e} \frac{v}{m_p} q_0 |\delta B_{ip}| \approx 7 \times 10^{-18} \left(\frac{10}{\xi_e} \right) \left(\frac{1 \text{ mHz}}{\nu} \right) \text{ m/s}^2 \sqrt{\text{Hz}} ; \quad (18)$$

Neither of these Lorentz-force magnetic effects is unacceptably large, even at 0.1 mHz. However, if it becomes impractical to discharge the PM more frequently than every few days, then the PM charge q could become larger than $q_0 \equiv 10^{-13}$ C, and A_4 could become significant enough to require greater electrostatic shielding. With this large a PM charge, other effects associated with the baseline capacitive sensors – A_{12} and A_{14} described below – would become even more significant. (See Table 2.)

Cosmic rays, particularly protons with energies E_{pr} in excess of about 200 MeV (3.2×10^{-11} J), will get stopped in the PM and impart momentum to it.[1] It is estimated that the rate n_{pr} at which this occurs will be about 30/sec.[1, 3] The average momentum imparted is $p = (m_{pr} E_{pr})^{1/2}$, where the proton mass is $m_{pr} = 1.7 \times 10^{-27}$ kg. The spectral density of the resulting acceleration disturbances is

$$A_5 \equiv \left(\frac{2n_{pr} m_{pr} E_{pr}}{m_p^2} \right)^{1/2} \approx 1.4 \times 10^{-18} \text{ m/s}^2 \sqrt{\text{Hz}} , \quad (19)$$

where the PM mass is $m_p = 1.3$ kg.

Impacts from residual gas in the PM housing may prove to be a greater problem. Opening the housing to space would permit the excellent vacuum needed to solve the problem, but would create problems of its own related to the opening mechanism. Assuming an average ambient temperature of 293°K and nitrogen molecules of mass $m_N = 4.65 \times 10^{-23}$ kg, the average thermal velocity of such a molecule will be

$$\bar{v} = \left(\frac{3k_B T_p}{m_N} \right)^{1/2} \approx 16 \text{ m/s} . \quad (20)$$

For an ambient residual gas pressure P , the number density of molecules $n = P/k_B T$ and the average impact rate w [s⁻¹] on any single side of the PM is

$$w = \frac{P A_p \bar{v}}{3k_B T_p} = \frac{P A_p}{(3m_N k_B T_p)^{1/2}} , \quad (21)$$

where the area A_p of each side of the PM is 1.6×10^{-3} m². Assuming Poisson statistics, the spectral density of fluctuations in w scales as $w^{1/2}$. Hence the spectral density of resulting acceleration disturbance to the PM is

$$A_6 \equiv \frac{P A_p}{m_p} \frac{\delta w}{w} = \frac{P A_p}{m_p w^{1/2}} = \frac{(P A_p)^{1/2}}{m_p} (3k_B T_p m_N)^{1/4} \approx 4.6 \times 10^{-16} \text{ m/s}^2 \sqrt{\text{Hz}} , \quad (22)$$

where the value given is for $P = 3 \times 10^{-7}$ Pa, or about 3×10^{-12} atmospheres. If the pressure were allowed to be larger, say 10^{-6} Pa, this magnitude of the disturbance would roughly double, making it one of the largest disturbance contributions. (See Table 2.)

The third impact-type of disturbance to the PM comes from laser photon radiation pressure. Intensity fluctuations δI in the laser output can easily be limited to one or two hundredths of a percent of the average power:

$$\delta I \equiv \eta I ; \quad \eta \approx 2 \times 10^{-4} / \sqrt{\text{Hz}} . \quad (23)$$

This value for η is, of course, much larger than the theoretical shot-noise limit $(2h\nu/I)^{1/2}$. The laser power incident on the PM will be about 10^{-4} W, so the resulting acceleration fluctuations for the PM are

$$A_7 \equiv \frac{2}{m_p c} \delta I \approx 10^{-16} \text{ m/s}^2 \sqrt{\text{Hz}} , \quad (24)$$

which are right about at the allowable limit.

Finally, there are several disturbances to the PM which arise from fluctuations in the temperature difference across the PM housing, or indirectly from temperature fluctuations across the SC which produce asymmetric distortions and consequent time-varying gravitational disturbances. First, there is a “radiometer” effect: a fluctuating temperature difference across the housing means unequal gas pressure and associated fluctuations. With a residual gas pressure $P = 3 \times 10^{-7}$ Pa and temperature fluctuations with spectral density $\delta T_p \approx 6 \times 10^{-5}$ K/ $\sqrt{\text{Hz}}$ [4], this effect will cause an acceleration disturbance

$$A_8 \equiv \frac{1}{2} \frac{A_p P}{m_p} \frac{\delta T_p}{T_p} \approx 4 \times 10^{-17} \left(\frac{\delta T_p}{6 \times 10^{-5} \text{K}/\sqrt{\text{Hz}}} \right) \text{ m/s}^2 \sqrt{\text{Hz}} . \quad (25)$$

If the pressure is larger than about 10^{-6} Pa, this disturbance would start to become a significant contributor. Since temperature stability across the PM is important for this contribution and even more so for that from thermal radiation pressure (see below), greater understanding of the actual thermal constant for the PM is needed (and will be dependent on the specific design). Since the PM thermal time constant will differ from that of the housing, it is possible that the relevant temperature stability may be better than estimated here.[4]

A second and larger thermal effect will come from fluctuations δW_p in the net thermal radiation pressure caused by fluctuations in the temperature difference across the PM housing. These fluctuations depend on the PM housing temperature T_p (about 293 K) and temperature variations δT_p by the Stefan-Boltzmann law,

$$\delta W_p = 4 \sigma T_p^3 \delta T_p \approx 3.4 \times 10^{-4} \left(\frac{\delta T_p}{6 \times 10^{-5} \text{K}/\sqrt{\text{Hz}}} \right) \text{ W/m}^2 \sqrt{\text{Hz}} , \quad (26)$$

where $\sigma \equiv 5.7 \times 10^{-8}$ W/ $\text{m}^2 \text{K}^4$. The resulting acceleration disturbance to the PM is estimated to be

$$A_9 \equiv \frac{2A_p}{3m_p c} \delta W_p \approx \frac{8\sigma A_p T_p^3}{3m_p c} \cdot \delta T_p \approx 9.4 \times 10^{-16} \left(\frac{\delta T_p}{6 \times 10^{-5} \text{K}/\sqrt{\text{Hz}}} \right) \text{ m/s}^2 \sqrt{\text{Hz}} . \quad (27)$$

The (much-needed) factor of one-third in this expression is an allowance for the fact that not all of the radiation momentum is normally incident on the PM, and derives from the fact that the radiation pressure for a Lambertian source is the energy density in the gap divided by three (*i.e.*, the integral of $\cos^2 \theta$).[9]

Temperature stability in the rest of the SC will not be nearly as good as the 6×10^{-5} K/ $\sqrt{\text{Hz}}$ assumed for the PM housing. Inherent fluctuations in the solar radiation flux [eq. (10) above], will produce temperature fluctuations at the SC as large as a few tenths of a degree/ $\sqrt{\text{Hz}}$:

$$\delta T_{sc} = \frac{T_{sc}}{4} \left(\frac{\delta W_0}{W_0} \right)_{srp} = \frac{T_{sc}}{4} \cdot 1.3 \times 10^{-3} \left(\frac{1 \text{ mHz}}{\nu} \right)^{1/3} \text{ Hz}^{-1/2} \approx 0.1 \text{ K}/\sqrt{\text{Hz}} \left(\frac{1 \text{ mHz}}{\nu} \right)^{1/3} , \quad (28)$$

where $T_{sc} \approx 293$ K. Passive thermal isolation will likely improve this by a couple of orders of magnitude, say to $\delta T_{sc} \leq 10^{-3}$ K/ $\sqrt{\text{Hz}}$. If most of the SC is aluminum with coefficient of thermal expansion (CTE) about 2.5×10^{-5} /K, then these temperature fluctuations could cause distortions $\delta x = x \cdot \text{CTE} |\delta T|$ as large as 12.5 nm/ $\sqrt{\text{Hz}}$ over distances x of about 0.5 m. The gravitational disturbance to the PM by a 1-kg piece of aluminum (“ M_{dis} ”) at a distance of 0.5 m that exhibits such distortions would be

$$A_{10} \equiv \frac{2GM_{dis}}{x^3} |\delta x| = \frac{2GM_{dis}}{x^2} \cdot (\text{CTE}) \cdot \delta T_{sc} \approx 1.4 \times 10^{-17} \left(\frac{1 \text{ mHz}}{\nu} \right)^{1/3} \text{ m/s}^2 \sqrt{\text{Hz}} . \quad (29)$$

The presence of nonzero voltages, capacitance, and PM charge leads to at least nine additional sources of spurious acceleration. Seven are derived in Appendix A and all are included in Tables 2 and 3. Four of them scale linearly with fluctuations in the displacement between the PM and its housing; these are discussed in the next subsection as part of the PM-SC coupling. The remaining five are given below in their approximate forms. (See Appendix A for more complete expressions.) Although more rigorous expressions will be obtained for specific sensor designs, the expressions below are considered realistic within factors of order unity for LISA’s currently baselined capacitive sensors. To estimate these expressions quantitatively, several assumptions are made, but the scaling factors are shown for easy conversion to other assumptions.

The gap d between PM and housing is 2 mm, and the gap asymmetry between opposite sides is $\Delta d \equiv d_{x1} - d_{x2} \approx 1 \mu\text{m}$. The average voltages across opposite sides, minus any voltage to ground, is $\frac{1}{2}(V_{x1} + V_{x2}) - V_g \equiv V_{x0} - V_g \approx 0.1 \text{ V}$. The difference in voltage across opposite sides is $\Delta V_x \equiv V_{x1} - V_{x2} \approx 0.01 \text{ V}$. The fluctuations in this voltage difference are assumed to be $\delta(\Delta V_x) \approx 10^{-5} \text{ V}/\sqrt{\text{Hz}}$. The capacitances $C_i \equiv \epsilon_0 A_p/d \approx 6 \text{ pF}$ for each side, leading to a total capacitance C of approximately $6C_i$ (or $7C_i$ if capacitance to ground C_g is comparable and included). The PM charge fluctuation δq , taken from eq. (16) above, is $1.3 \times 10^{-16} (1 \text{ mHz}/\nu) C/\sqrt{\text{Hz}}$. The maximum charge build-up on the PM will be taken to be $q_0 \equiv 10^{-13} \text{ C}$.

The first direct sensor disturbance, and the largest at 1 mHz, arises from fluctuations of the electrostatic forces associated with sensing and thus is quadratic in the sensor voltages and voltage fluctuations (eq. A17). It is assumed here that the larger voltages that may be necessary for PM position control within the housing will not exist most of the time and are not considered here as a steady-state contribution to PM acceleration fluctuations.

$$\begin{aligned} A_{11} &\equiv \frac{1}{m_p} \frac{C_x}{d} \frac{C_g}{C} (V_{x0} - V_g) \left[\delta(\Delta V_x) - \frac{\Delta d}{d} \delta V_i \right] \\ &\approx 39 \times 10^{-17} \text{ m/s}^2 \sqrt{\text{Hz}} \left(\frac{6C_g}{C} \right) \left(\frac{V_{x0} - V_g}{0.1 \text{ V}} \right) \left(\frac{\delta(\Delta V_x)}{10^{-5} \text{ V}/\sqrt{\text{Hz}}} \right). \end{aligned} \quad (30)$$

The second and third direct sensor disturbances arise from fluctuations of the interaction forces between net free charge on the PM and the applied sensing voltages (eqs. A18, A19).

$$\begin{aligned} A_{12} &\equiv \frac{1}{m_p} \frac{q}{d} \frac{C_x}{C} \left[\delta(\Delta V_x) - \frac{\Delta d}{d} \delta V_i \right] \\ &\approx 6.4 \times 10^{-17} \text{ m/s}^2 \sqrt{\text{Hz}} \left(\frac{q}{q_0} \right) \left[\left(\frac{\delta(\Delta V_x)}{10^{-5} \text{ V}/\sqrt{\text{Hz}}} \right) - 5 \times 10^{-4} \left(\frac{\Delta d}{1 \mu\text{m}} \right) \left(\frac{\delta V_i}{10^{-5} \text{ V}/\sqrt{\text{Hz}}} \right) \right]. \end{aligned} \quad (31)$$

$$\begin{aligned} A_{13} &\equiv \frac{1}{m_p d} \frac{C_x}{C} \left[\Delta V_x + \frac{\Delta d}{d} \frac{C_g}{C} (V_{x0} - V_g) \right] \delta q \\ &\approx 8.3 \times 10^{-17} \text{ m/s}^2 \sqrt{\text{Hz}} \left[\left(\frac{\Delta V_x}{0.01 \text{ V}} \right) + 8.3 \times 10^{-4} \left(\frac{6C_g}{C} \right) \left(\frac{V_{x0} - V_g}{0.1 \text{ V}} \right) \right] \left(\frac{1 \text{ mHz}}{\nu} \right). \end{aligned} \quad (32)$$

The fourth direct sensor disturbance arises from fluctuations of the interaction of the net free charge with the surrounding electrodes (eq. A20).

$$\begin{aligned} A_{14} &\equiv \frac{q}{m_p d} \frac{C_x}{C^2} \frac{\Delta d}{d} \delta q \\ &\approx 1.2 \times 10^{-20} \text{ m/s}^2 \sqrt{\text{Hz}} \left(\frac{q}{q_0} \right) \left(\frac{\Delta d}{1 \mu\text{m}} \right) \left(\frac{1 \text{ mHz}}{\nu} \right). \end{aligned} \quad (33)$$

Finally, additional noise arises due to the (digital-to-analog) quantization process associated with adjustments in the sensing voltage. If one assumes that the maximum range of voltage adjustment corresponds to no more than about 10 times the average force F_{x0} exerted for sensing (which is shown in eq. A9 to be about $4.2 \times 10^{-13} \text{ N}$), then, for $N = 16$ bits and sampling frequency f_s of about 100 Hz, this quantization noise is approximately

$$A_{15} \equiv \frac{10F_{x0}}{m_p} \frac{1}{2^N} \frac{1}{\sqrt{12}f_s} \approx 1.4 \times 10^{-18} \text{ m/s}^2 \sqrt{\text{Hz}}. \quad (34)$$

Comparison with the other acceleration disturbances (see Table 2) shows that some of these effects are potentially among the largest in the LISA budget. All would benefit from a larger gap d , provided that does not result in a still larger requirement for the average electrode voltage V_{x0} (A_{11} , A_{15}). The two that depend significantly on the PM net free charge q (A_{12} and A_{14}) could be reduced by discharging the PM more often, to ensure that the net charge remains smaller than 10^{-13} C . The third one, A_{13} , proportional to the product of charge fluctuations and voltage difference across opposite electrodes, could probably only be reliably reduced by increasing the gap, since it could be significant even in the absence of applied voltages, if the

inherent contact potentials (“patch fields”) that exist on inside faces of the PM housing (along the sensitive axis) are as large as 0.01 V, which is considered a possibility.[5,6,9, 12] Furthermore, this effect will begin to dominate the entire LISA acceleration disturbance budget at frequencies of 0.1 mHz and lower. As shown in the next section, these contact potentials may also cause large contributions to the coupling between PM and SC, especially at low frequencies. Analytic and laboratory studies are underway to understand the magnitudes, relevant length scales, and temporal properties of these contact potentials.[17] It is also important to verify eq. (16) for the expected charging rate. If both of these factors turn out to be as large as the assumptions herein, a larger gap may be imperative.

Estimates of the PM disturbances described above as A_1 through A_{15} are summarized in Table 2, with the key assumptions noted therein. With those assumptions, after adding in quadrature all the contributions, the rss total PM “direct” acceleration disturbance is about $1.13 \times 10^{-15} \text{ m/s}^2\sqrt{\text{Hz}}$ at 10 mHz and 1 mHz, and about $1.42 \times 10^{-15} \text{ m/s}^2\sqrt{\text{Hz}}$ at 0.1 mHz. At frequencies of 1 mHz and higher, the dominant sources of spurious acceleration are thermal radiation pressure (A_9), residual gas pressure (A_6), and the interaction of average voltages and voltage-difference fluctuations in the capacitive sensor (A_{11}). Only the last of these is ameliorated by using a larger gap. At 0.1 mHz and lower, a second sensor-related disturbance begins to dominate, that caused by the interaction of PM charge fluctuation with the voltage difference across opposite faces of the PM (A_{13}); this disturbance could be reduced somewhat with a larger gap. The results summarized in Table 2 may be compared with the preliminary budget for acceleration noise presented in [1], Table 4.2, which allows a total of $3 \times 10^{-15} \text{ m/s}^2\sqrt{\text{Hz}}$ at 0.1 mHz for each PM displacement sensor. This table is reproduced here for reference, following Appendix A.

Referring back to eqs. (9) for the total PM acceleration disturbance A_p , it is apparent that two of the five quantities to be determined have now been estimated. The total “external” SC acceleration disturbance $A_{ns} + TN_t$ was estimated in eq. (12), and the total “direct” PM acceleration disturbance A_{np} is the rss of the quantities A_1 through A_{15} above. It remains to estimate the PM-SC coupling constant K . Then, by requiring that the total PM acceleration disturbance be smaller than the goal of $3 \times 10^{-15} \text{ m/s}^2\sqrt{\text{Hz}}$, requirements can be inferred for the SC control-loop gain u and the displacement sensor sensitivity X_{nr} .

4.3 Proof Mass - Spacecraft Coupling

The PM-SC coupling has two basic origins. One is gravitational force gradients. These are different from the time-varying gravitational force fluctuations A_{10} described above, which arise primarily from thermal-caused distortion or motion. In the approximation that the PM housing is rigidly coupled to the rest of the SC, gravitational-gradient disturbances arise with any fluctuation in the separation X_{ps} between the PM and its housing. For a given “disturbing mass” M_{dis} at a distance r from the PM, where $r < 1$ m, the amplitude of the acceleration disturbance to the PM caused by a fluctuation X_{ps} in the “gap” is

$$A_{gg} = 2G \left(\frac{M_{dis}}{r^3} \right) X_{ps} \equiv K_{gg} X_{ps} , \quad (35)$$

where $G \equiv 6.7 \times 10^{-11} \text{ m}^3/\text{kg}\cdot\text{s}^2$. This assumes the worst-case situation, where the motion is entirely along the sensitive axis. Typical disturbing masses will be less than about 5 kg. Using $r = 0.5$ m gives

$$K_{gg} \approx 5 \times 10^{-9} / \text{s}^2 . \quad (36)$$

If this were the entire contribution to the coupling, the rss of the three terms that comprise the total PM acceleration disturbance A_p could be kept below the nominal goal of $3 \times 10^{-15} \text{ m/s}^2\sqrt{\text{Hz}}$ at 1 mHz with a dimensionless SC control-loop gain of only 20 and a displacement sensor sensitivity of only $200 \text{ nm}/\sqrt{\text{Hz}}$, according to eqs. (9) and (12) and the estimates for A_{np} above. Unfortunately, the sensor itself contributes to the coupling. However, as shown below, with certain assumptions that are plausible but have yet to be demonstrated, it appears that capacitive sensors might be made that will contribute a net amount to the PM-SC coupling that is not larger than that due to gravitational gradients.

A capacitive sensor contributes to the PM-SC coupling in at least four estimable ways, all of which arise through gradients of the capacitances or their derivatives. These are derived in Appendix A. Since to first order the forces scale linearly with fluctuations X_{ps} in the separation between the PM and its housing, they can be viewed as contributing linearly to the total PM-SC coupling constant K . One contribution arises

from fluctuations in the Coulomb interaction between the charged PM and image charges on the surrounding metal electrodes:

$$\begin{aligned} K_{s1} &= \frac{1}{m_p} \left[\frac{1}{2C^2} q^2 \sum_i \frac{\delta C'_i}{\delta x} - (V'_m)_2 \frac{q}{C} \sum_i \frac{\delta C_i}{\delta x} \right] \\ &\approx \frac{1}{m_p C d^2} \left(\frac{C_x}{C} \right) q^2 \approx 9 \times 10^{-12} / s^2 \left(\frac{q}{q_0} \right)^2, \end{aligned} \quad (37)$$

where the notation and assumptions are described in Appendix A [see eq. (A.23)]. This coupling scales quadratically with the net charge q on the PM and linearly with the inverse of the gap d . While this appears to be significantly smaller than that estimated for gravitational force gradients, it is highly dependent on limiting the net charge on the PM.

A second sensor contribution to the PM-SC coupling arises from interaction between the net free charge q on the PM and the average electrode voltages *via* changes in capacitance gradients that arise from fluctuations in the gap. This coupling scales linearly with the PM charge q and average voltage $V_{x0} - V_g$ on opposing electrodes (minus any voltage V_g to ground), and quadratically with the inverse of the gap d :

$$\begin{aligned} K_{s2} &= \frac{1}{m_p} \frac{-q}{C} \sum_i \frac{\delta C'_i}{\delta x} (V_i - V_s) \\ &\approx -\frac{2}{m_p d^2} \left(\frac{C_x}{C} \right) \left(\frac{C_g}{c} \right) q (V_{x0} - V_g) \approx 10^{-10} / s^2 \left(\frac{6C_g}{C} \right) \left(\frac{V_{x0} - V_g}{0.1 \text{ V}} \right) \left(\frac{q}{q_0} \right), \end{aligned} \quad (38)$$

where a maximum charge of $q_0 \equiv 10^{-13}$ C has been assumed. This contribution also is much smaller than the gravitational-gradient coupling, provided the net charge on the PM is kept suitably small. Its quadratic dependence on the inverse of the gap d would allow it to be suppressed by an increase in the gap.

A third sensor coupling contribution scales with the squares of both the average voltages across electrodes and the voltage difference across opposite electrodes. It, too, is smaller than the gravitational gradient contribution, with the assumptions noted for the average voltage and voltage differences:

$$\begin{aligned} K_{s3} &= \frac{1}{m_p} \left[(V'_m)_1 \sum_i \frac{\delta C_i}{\delta x} (V_i - V_s) + \frac{1}{2} \sum_i \frac{\delta C'_i}{\delta x} (V_i - V_s)^2 \right] \\ &\approx \frac{1}{m_p} \frac{C_x}{d^2} \left[\frac{C_x}{C} (\Delta V_x)^2 + \left(\frac{C_g}{C} \right)^2 (V_{x0} - V_g)^2 + \frac{1}{4} (\Delta V_x)^2 \right] \\ &\approx 3.4 \times 10^{-10} / s^2 \left[0.94 \left(\frac{V_{x0} - V_g}{0.1 \text{ V}} \right)^2 + 0.06 \left(\frac{\Delta V_x}{0.01 \text{ V}} \right)^2 \right]. \end{aligned} \quad (39)$$

The assumption of 0.1 V for the average voltage across electrodes on opposite sides of the PM may be optimistic for the sensing sensitivity desired, but it is probably realistic within a factor of two. However, even in the absence of applied voltages, there are likely to exist ‘‘patch-field’’ voltages on the electrode surfaces, thought to arise from local variations in the electrochemical potential across the surface of the metal.[5,6] The magnitude of the variations can be reduced through control of surface cleanliness and chemical contamination, but inherent impurities associated with boundaries between crystallite planes or slight variations in alloy concentrations can still produce effective variations as large as tens of or perhaps a hundred millivolts. While the magnitudes and controllability of these effects require further study, worst-case estimates of plausible scenarios give an rms magnitude for the patch-field voltage $V_{pe} \approx 0.1$ V and an overall multiplicative factor γ as large as 5, essentially cancelling the effect of $C_x/C \approx 1/6$ included in the expression above for K_{s3} . This would give a patch-effect contribution to the PM-SC coupling that is roughly five times larger than K_{s3} :

$$K_{s4} \approx 1.6 \times 10^{-9} / s^2 \left(\frac{V_{pe}}{0.1 \text{ V}} \right)^2. \quad (40)$$

While this contribution could be the largest from the capacitive sensor, and is largely uncontrollable except by increasing the gap, it is still less than half that of the gravitational gradient. The rss of these five contributions to the PM-SC coupling strength K [eqs. (35)–(39)] is

$$K \equiv \text{rss}\{K_{gg}, K_{s1}, \dots, K_{s4}\} \approx 5.3 \times 10^{-9} / s^2. \quad (41)$$

Estimates of the PM-SC coupling strength described above are summarized in Table 3, with key assumptions denoted therein.

5 Summary

Tables 1, 2, and 3 provide summaries of the estimates made above. Table 4 is a summary of numerical assumptions for parameters included in the estimates. In Table 1C, the “external” SC disturbances $A_{ns} + TN_t$ were estimated to contribute acceleration fluctuations of $3.4 \times 10^{-10} \text{ m/s}^2\sqrt{\text{Hz}}$ at $\omega/2\pi = 1 \text{ mHz}$, and about 35% larger at 0.1 mHz. The PM “direct” disturbances A_{np} were estimated at $1.13 \times 10^{-15} \text{ m/s}^2\sqrt{\text{Hz}}$ at 1 mHz and $1.42 \times 10^{-15} \text{ m/s}^2\sqrt{\text{Hz}}$ at 0.1 mHz, as explained above. The larger value at 0.1 mHz arises primarily from coupling of PM charge fluctuations to the voltage difference across opposite sides of the PM (A_{11}), and it includes assumptions on the charging rate and its $1/\nu$ frequency dependence. The total coupling constant K was estimated to be an ambitious $5.3 \times 10^{-9}/\text{s}^2$, dominated by gravitational gradients. In Table 1D, requirements are inferred for the sensor readout sensitivity X_{nr} and the SC drag-free control loop gain u by requiring that each of their contributions to the total PM acceleration disturbance A_p be no larger than $1.5 \times 10^{-15} \text{ m/s}^2\sqrt{\text{Hz}}$, which guarantees that the rss of all three contributions will meet the LISA requirement. This results in the requirements that the readout sensitivity be at least as good as $280 \text{ nm}/\sqrt{\text{Hz}}$ at all frequencies, and the SC drag-free control loop gain u be at least 30 at 1 mHz and more than 4100 at 0.1 mHz. Note that the nominal requirement for readout sensitivity given in [1, Table 3.3 therein] was $2.5 \text{ nm}/\sqrt{\text{Hz}}$.

The above analysis reveals where deeper understanding and more careful error assessments are needed, and where possible tradeoffs might be considered. While these estimates are approximate and likely do not reflect the depth or detail that may exist in various organizations actively working on LISA in Europe and the U.S., it is hoped that this presentation will provide at least heuristic benefit for the uninitiated and perhaps a basis for discussion and improved understanding for those actively involved in analysis, modelling, and experimental efforts.

Table 1: LISA Acceleration Disturbances and Requirements

1A. Definitions (See Eqs. 1-9 in text.)

A_p	$\text{m/s}^2\sqrt{\text{Hz}}$	PM acceleration disturbance $\equiv \text{rss} [A_{np}, (A_{ns} + TN_t) K/\omega^2 u, KX_{nr}]$
X_p	$\text{m}/\sqrt{\text{Hz}}$	PM position disturbance $\equiv A_p/\omega^2$
A_{np}	$\text{m/s}^2\sqrt{\text{Hz}}$	PM direct acceleration disturbances
$A_{ns} + TN_t$	$\text{m/s}^2\sqrt{\text{Hz}}$	SC external acceleration disturbances (solar flux & thruster noise)
$K \equiv \omega_0^2$	s^{-2}	PM-SC coupling constant
$v \equiv K/\omega^2$	[1]	Dimensionless PM-SC spring constant ($v \ll 1$)
$K_r \equiv \omega_r^2$	s^{-2}	PM displacement readout stiffness
$u \equiv TK_r/\omega^2$	[1]	SC drag-free control-loop gain ($u \gg 1$)
X_{nr}	$\text{m}/\sqrt{\text{Hz}}$	Displacement sensor readout sensitivity

1B. LISA DRS Goals (per PM)

$\omega/2\pi$:	$3 \times 10^{-3} \text{ Hz}$	10^{-3} Hz	10^{-4} Hz	
A_p	$10^{-15} \text{ m/s}^2\sqrt{\text{Hz}}$	3	3	3
$X_p \equiv A_p/\omega^2$	$10^{-12} \text{ m}/\sqrt{\text{Hz}}$	10	80	8000

1C. Estimated contributions to A_p and X_p

$\omega/2\pi$:	$3 \times 10^{-3} \text{ Hz}$	10^{-3} Hz	10^{-4} Hz	
A_{np} (eqs. 13-34)	$10^{-15} \text{ m/s}^2\sqrt{\text{Hz}}$	1.13	1.13	1.42
$X_{np} \equiv A_{np}/\omega^2$	$10^{-12} \text{ m}/\sqrt{\text{Hz}}$	3	30	3600
$A_{ns} + TN_t$ (eq. 12)	$10^{-15} \text{ m/s}^2\sqrt{\text{Hz}}$	3.2×10^5	3.4×10^5	4.6×10^5
$X_{ns} \equiv (A_{ns} + TN_t)/\omega^2$	$10^{-6} \text{ m}/\sqrt{\text{Hz}}$	1	10	1200
K (eq.41)	s^{-2}	5.3×10^{-9}	5.3×10^{-9}	5.3×10^{-9}
$v \equiv K/\omega^2$	[1]	1.5×10^{-5}	1.34×10^{-4}	1.34×10^{-2}

1D. Minimum[†] requirements to meet LISA goal of $A_p \leq 3 \times 10^{-15} \text{ m/s}^2\sqrt{\text{Hz}}$

$\omega/2\pi$:	$3 \times 10^{-3} \text{ Hz}$	10^{-3} Hz	10^{-4} Hz
u	3	30	4100
X_{nr}	$10^{-9} \text{ m}/\sqrt{\text{Hz}}$	280	280

[†] Values for X_{nr} and u are chosen to make each of their respective contributions to A_p no larger than $1.5 \times 10^{-15} \text{ m/s}^2\sqrt{\text{Hz}}$, resulting in a final rss value for A_p that is $\leq 2.6 \times 10^{-15} \text{ m/s}^2\sqrt{\text{Hz}}$.

Table 2: PM “direct” acceleration disturbances

Contributions to A_{np} [10^{-17} m/s²√Hz] (See Eqs. 13-34 in text.)

A_1	Magnetic	$\frac{6\chi_m}{\rho\mu_0\xi_m r_{sc}} B_{sc} \delta B_{sc}$	$1.2 \left(\frac{1}{\xi_m} \right)$
A_2	Magnetic	$\frac{3\chi_m}{\rho\mu_0\xi_m r_{sc}} B_{sc} \delta B_{ip}$	$2.5 \left(\frac{1}{\xi_m} \right) \left(\frac{1 \text{ mHz}}{\nu} \right)$
A_3	Magnetic	$\frac{v}{\xi_e m_p} \delta q B_{ip}$	$0.01 \left(\frac{10}{\xi_e} \right) \left(\frac{1 \text{ mHz}}{\nu} \right)$
A_4	Magnetic	$\frac{v}{\xi_e m_p} q \delta B_{ip}$	$0.7 \left(\frac{10}{\xi_e} \right) \left(\frac{q}{q_0} \right) \left(\frac{1 \text{ mHz}}{\nu} \right)$
A_5	Cosmic rays ¹	$\frac{1}{m_p} (2n_{pr} m_{pr} E_{pr})^{1/2}$	$0.14 \left(\frac{E_{pr}}{200 \text{ MeV}} \right)^{1/2}$
A_6^*	Residual gas ²	$\frac{1}{m_p} (PA_p)^{1/2} (3k_B T_p m_N)^{1/4}$	$46 \left(\frac{P}{3 \times 10^{-7} \text{ Pa}} \right)^{1/2}$
A_7^*	Laser photons	$\frac{2}{m_p c} \delta I$	$10 \left(\frac{\delta I}{2 \times 10^{-8} \text{ W}/\sqrt{\text{Hz}}} \right)$
A_8	Radiometric	$\frac{A_p P}{2m_p T_p} \delta T_p$	$4 \left(\frac{P}{3 \times 10^{-7} \text{ Pa}} \right) \left(\frac{\delta T_p}{6 \times 10^{-5} \text{ K}/\sqrt{\text{Hz}}} \right)$
A_9^*	Thermal Rad'n Press	$\frac{8}{3} \frac{\sigma A_p}{m_p c} T_p^3 \delta T_p$	$94 \left(\frac{\delta T_p}{6 \times 10^{-5} \text{ K}/\sqrt{\text{Hz}}} \right)$
A_{10}	Grav. thermal distortion ³	$\frac{2GM_{dis}}{x^2} \cdot CTE \cdot \delta T_{sc}$	$1.4 \left(\frac{\delta T_{sc}}{10^{-3} \text{ K}/\sqrt{\text{Hz}}} \right) \left(\frac{1 \text{ mHz}}{\nu} \right)^{1/3}$
rss ($A_1 - A_{10}$) = 105 at 10 mHz and 1 mHz, 108 at 0.1 mHz			
A_{11}^*	Voltage fluct'ns × voltage ⁴	$\approx \frac{C_x}{m_p d} \frac{C_g}{C} (V_{x0} - V_g) \delta(\Delta V_x)$	$39 \left(\frac{\delta(\Delta V_x)}{10^{-5} \text{ V}/\sqrt{\text{Hz}}} \right) \left(\frac{6C_g}{C} \right) \left(\frac{V_{x0} - V_g}{0.1 \text{ V}} \right)$
A_{12}	Voltage fluct'ns × charge ⁴	$\approx \frac{1}{m_p d} \frac{C_x}{C} q \delta(\Delta V_x)$	$6.4 \left(\frac{\delta(\Delta V_x)}{10^{-5} \text{ V}/\sqrt{\text{Hz}}} \right) \left(\frac{q}{q_0} \right)$
A_{13}^*	Charge fluct'ns × voltage	$\approx \frac{1}{m_p d} \frac{C_x}{C} \Delta V_x \delta q$	$8.3 \left(\frac{\Delta V_x}{0.01 \text{ V}} \right) \left(\frac{1 \text{ mHz}}{\nu} \right)$
A_{14}	Charge fluct'ns × charge ⁵	$\approx \frac{1}{m_p d} \frac{C_x}{C^2} \frac{\Delta d}{d} q \delta q$	$0.0012 \left(\frac{\Delta d}{1 \mu\text{m}} \right) \left(\frac{1 \text{ mHz}}{\nu} \right)$
A_{15}	Voltage Quantization ⁶	$\frac{10F_{x0}}{m_p} \frac{1}{2N} \frac{1}{\sqrt{12f_s}}$	$0.14 \left(\frac{F_{x0}}{4.2 \times 10^{-13} \text{ N}} \right) \left(\frac{100 \text{ Hz}}{f_s} \right)$
rss ($A_1 - A_{15}$) = 113 at 10 and 1 mHz, 142 at 0.1 mHz			

* Largest contributors (under stated assumptions)

¹ $n_{pr} \approx 30/\text{sec}$ for $E_{pr} \geq 200 \text{ MeV}$ ($3.2 \times 10^{-11} \text{ J}$); $m_{pr} = 1.7 \times 10^{-27} \text{ kg}$.

² $m_N = 4.65 \times 10^{-23} \text{ kg}$ (nitrogen molecules, N_2).

³ $M_{dis} \approx 1 \text{ kg}$, $x \approx 0.5 \text{ m}$; CTE of aluminum $\approx 2.5 \times 10^{-5}/\text{K}$.

⁴ $\Delta V_x \equiv |V_{x1} - V_{x2}| =$ voltage difference across opposite faces along x -axis (and other axes).

$\delta(\Delta V_x) \equiv$ fluctuations in voltage difference across opposite faces .

$V_{x0} \equiv (V_{x1} + V_{x2})/2 \equiv$ average voltage across opposite faces.

$C_g (V_g) \equiv$ capacitance (voltage) to ground.

$C_x \equiv \epsilon_0 A_p/d \approx 6 \text{ pF}$; $C \approx 6 C_x$; $C' \approx (C_x/d^2) \Delta d \approx 1.5 \text{ pF/m}$ ($\Delta d/1 \mu\text{m}$).

$\Delta d \equiv$ asymmetry in gap across opposite sides of PM ($= d_{x1} - d_{x2}$).

⁵ $\delta q \equiv (2e\dot{q})^{1/2}/\omega \approx 1.3 \times 10^{-16} (1 \text{ mHz}/\nu) C/\sqrt{\text{Hz}}$, $\dot{q} \approx 13 e/\text{sec}$ from cosmic rays (eq. 16).

⁶ $N = 16$, $f_s = 100 \text{ Hz}$; F_{x0} from eq. A.9.

Table 3: PM-SC Coupling

Contributions to K [$10^{-9} /(\text{s}^2)$] (See Eqs. 35-41 in text.)

K_{gg}	Gravitational gradients	$2G \frac{M_{dis}}{r^3}$	$5 \left(\frac{M_{dis}}{5 \text{ kg}} \right) \left(\frac{0.5 \text{ m}}{r} \right)^3$
K_{s1}	Coulomb - Image charges	$\frac{1}{m_p C d^2} \left(\frac{C_x}{C} \right) q^2$	$0.009 \left(\frac{q}{q_0} \right)^2$
K_{s2}	PM charge \times voltage	$\left(\frac{2}{m_p d^2} \right) \left(\frac{C_x}{C} \right) \left(\frac{C_g}{C} \right) q (V_{x0} - V_g)$	$0.1 \left(\frac{6C_g}{C} \right) \left(\frac{V_{x0} - V_g}{0.1 \text{ V}} \right) \left(\frac{q}{q_0} \right)$
K_{s3}	Applied voltages	$\frac{C_x}{m_p d^2} \left[\left(\frac{C_x}{C} \right) \Delta V_x \right]^2 + \left(\frac{C_g}{C} \right)^2 (V_{x0} - V_g)^2$	$0.34 \left(\frac{V_{x0} - V_g}{0.1 \text{ V}} \right)^2$
K_{s4}	Patch-field voltages	$\gamma \left(\frac{C_x}{m_p d^2} \right) \left(\frac{C_g}{C} \right)^2 \left(\frac{V_{pe}}{0.1 \text{ V}} \right)^2$	$1.6 \left(\frac{\gamma}{5} \right) \left(\frac{V_{pe}}{0.1 \text{ V}} \right)^2$
$\text{rss} \equiv K = 5.3 \times 10^{-9} / \text{s}^2$			

Table 4: Numerical assumptions for DRS estimates

<p>Spacecraft: $M_{sc} = 300$ kg $A_{sc} = 4$ m² \equiv area of SC facing the sun $r_{sc} \approx 1$ m $T_{sc} \approx 293$ K CTE (Aluminum) $\approx 2.5 \times 10^{-5}/K$ $v \approx 3 \times 10^4$ m/s ≈ 1 au ($2\pi/1$ yr) $B_{sc} \approx 7 \times 10^{-6}$ T (Tesla) (modeled as dipole of magnitude 1 A-m² at $r \approx 0.35$ m from PM, caused by permanent magnets mounted on lasers [8]) $\delta B_{sc} \approx 7 \times 10^{-9}$ T/$\sqrt{\text{Hz}}$ $B_{ip} \approx 3 \times 10^{-7}$ T $\delta B_{ip} \approx 3 \times 10^{-8}(1 \text{ mHz}/\nu)$ T/$\sqrt{\text{Hz}}$</p>
<p>Proof Mass & Housing: $m_p = 1.3$ kg (Pt-Au, 10%-90%) $A_p = 1.6 \times 10^{-3}$ m² \equiv area of (cubical) PM $\rho = 2 \times 10^4$ kg/m³ = 20 gm/cm³ $\chi_m \approx 10^{-6}$ \equiv magnetic susceptibility for Pt-Au (10%-90%) $q_0 = 10^{-13}$ C \equiv maximum charge build-up on the PM $d = 2$ mm \equiv “gap” between PM and electrodes (sensitive axis) $T_p = 293$ K ; $P \approx 3 \times 10^{-7}$ Pa . ξ_m (ξ_e) \equiv magnetic (electrostatic) shielding factor</p>
<p>Laser: $\delta I/I \approx 2 \times 10^{-4}$ \equiv relative intensity fluctuations</p>
<p>Physical Constants $\mu_0 = 1.26 \times 10^{-6}$ N/A² \equiv permeability of vacuum $\sigma = 5.7 \times 10^{-8}$ W/m²K⁴ \equiv Stefan-Boltzmann constant $G = 6.7 \times 10^{-11}$ m³/kg - s² \equiv gravitational constant $k_B = 1.38 \times 10^{-23}$ J/K \equiv Boltzmann constant $\epsilon_0 = 8.9 \times 10^{-12}$ F/m \equiv permittivity of vacuum 1 au $\equiv 1.5 \times 10^{11}$ m $c \approx 3 \times 10^8$ m/s \equiv speed of light in vacuum</p>

6 References

1. System and Technology Study Report for LISA: Laser Interferometer Space Antenna, A Cornerstone Mission for the observation of gravitational waves, ESA-SCI(2000) **11**, (July 2000).
2. LISA Integrated Modeling Plan, R. T. Stebbins, *et al.*, draft (October 2001).
3. Y. Jafry and T.J.Sumner, *Electrostatic charging of the LISA proof masses*, Class. Quantum Grav., **14** (1997), 1567-1574.
4. Final Technical Report of the (Phase A) Study of the Laser Interferometer Space Antenna (Dornier Satellitensysteme GmbH - Matra Marconi Space - Alenia Aerospazio), ESTEC Contract No. 13631/99/NL/MS, Report No. LI-RP-DS-009 (April 2000).
5. J. B. Camp, T. W. Darling, and Ronald E. Brown, *Effect of crystallites on surface potential variations of Au and graphite*, J. Appl. Phys. **71** (1992), 783-785.
6. C. C. Speake, *Forces and force gradients due to patch fields and contact-potential differences*, Class. Quantum Grav. **13** (1996), A291-A297.
7. C. C. Speake and P. L. Andrews, *Capacitive sensing for drag-free satellites*, Class. Quantum Grav. **14** (1997), 1557-1565.
8. M. Rodrigues and P. Touboul, *Optimisation of the inertial sensor design for the LISA mission*, ONERA Technical Report #RTS 24/3815 DMPH/Y (July 1998).
9. P.Bender, private communication (December 2001), notes that a 20-Amp current (I) flowing around a 1-m diameter circle ($\rho \equiv 0.5$), with the return current flowing back around a concentric circle of radius differing by, say 2 mm ($\equiv d$), produces a dc magnetic field 25 cm away ($\equiv z$) whose magnitude is no larger than 10^{-7} T ($|B| \approx \mu_0 I d \rho / 2r^3$ to first-order in d/ρ and z/ρ , where $r^2 \equiv \rho^2 + z^2$). A more rigorous calculation reduces this to about 20 nT, using the Biot-Savart law, $d\vec{B} = (\mu_0 I / 4\pi r^3) d\vec{l} \times \vec{r}$.
10. L. Landau and E. Lifshitz, *Electrodynamics of Continuous Media*, Addison-Wesley (1960), Chapters 2 and 5.
11. S. Vitale, private communication (March 2002).
12. S. Vitale, *Note on effect of contact potential and charging*, draft (December 8, 2001).
13. A. Abramovici, M. Chiao, *et al.*, private communication (October 2001).
14. J. Pap, *et al.*, *Variations in total solar and spectral irradiance as measured by the VIRGO experiment on SOHO*, Adv. Space Res. **24**, No. 2 (1999), 215-224.
15. J. Ziemer, J. Mueller, private communication (December 2001).
16. Y. Su, *et al.*, *New tests of the universality of free fall*, Physical Review D **50** (1994), 3614-3636).
17. J. Camp, private communication (March 2002).
18. R. Spero, private communication (2002); *Reference Data for Radio Engineers*, 1972.

7 Appendix A: Capacitive Sensor-induced Disturbances

Following a description used in reference [1], consider the PM and its surrounding electrodes as a bank of capacitors surrounding the PM, which forms a common central electrode. The total capacitance of the arrangement is

$$C \equiv \sum_i C_i, \quad i = x_1, x_2, y_1, y_2, z_1, z_2, g, \quad (\text{A.1})$$

where the different subscripts i refer to the six sides of the (cubical) PM plus any stray capacitance to ground, C_g . The PM acquires a potential V_s from potentials V_i on the surrounding electrodes, where the V_i include applied voltages as well as average differences between the work functions on the electrodes and facing sides of the PM (“contact potentials” or patch-effect voltages). Thus,

$$V_s \equiv C^{-1} \sum_i V_i C_i. \quad (\text{A.2})$$

As the PM acquires a net free charge q , the total mechanical energy W of the arrangement can be expressed as

$$\begin{aligned} W &= -\frac{1}{2} \sum_i C_i (V_i - V_s)^2 + \frac{1}{2} \frac{q^2}{C} + qV_s \\ &= -\frac{1}{2} \sum_i C_i (V_i - V_m)^2 + qV_m, \end{aligned} \quad (\text{A.3})$$

where

$$V_m \equiv V_s + \frac{q}{C}. \quad (\text{A.4})$$

The minus sign for the first term in each expression for W results from inclusion of the energy provided by the charge reservoirs (batteries) in keeping the applied voltages constant.[10,11] (The sign would be positive for electrodes with constant charge.) It will be useful to write the derivative of V_m as the sum of two functions, the second of which contains all the dependence on net free charge q :

$$V'_m = \frac{1}{C} \sum_i C'_i (V_i - V_m) = \frac{1}{C} \sum_i C'_i (V_i - V_s) - \frac{q}{C^2} \sum_i C'_i \equiv (V'_m)_1 + (V'_m)_2, \quad (\text{A.5})$$

where a prime denotes gradient along the sensitive (x -) axis. Using this relation, one can write the net force F_x on the PM along the x -axis as

$$F_x = -\partial_x W = \frac{1}{2} \sum_i C'_i (V_i - V_m)^2 + \sum_i C_i V'_i (V_i - V_m) - V_m q'. \quad (\text{A.6})$$

In the approximation that neither the free charge q nor the potentials V_i have appreciable gradients along the x -axis, the net force reduces to the first term alone, which can be rewritten in terms of the PM potential V_s and net free charge q using the definition of V_m as follows:

$$F_{x0} \equiv \frac{1}{2} \sum_i C'_i (V_i - V_m)^2 = \frac{1}{2} \sum_i C'_i (V_i - V_s)^2 + \frac{1}{2} C' \frac{q^2}{C^2} - \frac{q}{C} \sum_i C'_i (V_i - V_s). \quad (\text{A.7})$$

Physically, these terms can be interpreted as follows: The first term, proportional to the square of applied voltages, represents electrostatic forces associated with suspension, control, and sensing. (For calculations of the acceleration disturbances, proportional not to the average force but to fluctuations in that force, it will be assumed that only the smaller sensing voltages exist to produce steady-state disturbances.) The second term arises from interaction of the free charge q with the surrounding electrodes; and the third term describes interaction between the free charge and the applied voltages.

It is usual to assume that only the capacitances $C_{x1} = C_{x2} \equiv C_x$ have nonzero gradients along the x -axis, and that these are opposite in sign but differ in magnitude by any asymmetry Δd in the gaps, *i.e.*,

$$\begin{aligned} C'_{x1} &\approx \frac{C_x}{d} \left(\frac{1}{1-\alpha} \right), \\ C'_{x2} &\approx \frac{C_x}{d} \left(\frac{1}{1+\alpha} \right), \end{aligned} \quad (\text{A.8})$$

where $\alpha \equiv \Delta d/2d$. In the approximation that there is no appreciable asymmetry in the PM-electrode gaps on opposing sides, and assuming that the voltage to ground is zero, $V_g \equiv 0$, the net force on the PM reduces to

$$\begin{aligned} F_{x0} &\approx \frac{C_x C_g}{2d C} (V_{x1}^2 - V_{x2}^2) - \frac{C_x q}{d C} (V_{x1} - V_{x2}) \\ &\approx 4.2 \times 10^{-13} \text{ N}, \end{aligned} \quad (\text{A.9})$$

where the numerical estimate assumes $C_x \approx 6$ pF, $C_g/C \approx 1/6$, $d = 2$ mm, $V_{x1} + V_{x2} \approx 0.2$ V, and $V_{x1} - V_{x2} \approx 0.01$ V. The general expression above for F_{x0} agrees with expressions derived elsewhere.[12] The calculations herein allow for an asymmetry in the gaps, but it will be seen that this contribution is almost negligible unless the gap asymmetry is on the order of 10 microns or larger.

Of special interest here is not the average force F_x on the PM, but rather the possible magnitude of fluctuations in that force, δF_x , which will cause acceleration disturbance to the PM. The full expression for the variation of the force in the x -direction, δF_x is:

$$\delta F_x = \delta F_{x,A} + \delta F_{x,K} + \delta F_{x,q'} + \delta F_{x,V'} , \quad (\text{A.10})$$

where

$$\begin{aligned} \delta F_{x,A} &\equiv \sum_i \delta V_i [C'_i (V_i - V_m) - C_i V'_m] - V'_m \delta q ; \\ \delta F_{x,K} &\equiv V'_m \sum_i \delta C_i (V_i - V_m) + \frac{1}{2} \sum_i \delta C'_i (V_i - V_m)^2 ; \\ \delta F_{x,q'} &\equiv -V_m \delta q' ; \\ \delta F_{x,V'} &\equiv \sum_i \delta V'_i C_i (V_i - V_m) + \sum_i V'_i [C_i \delta V_i + \delta C_i (V_i - V_m)] . \end{aligned} \quad (\text{A.11})$$

In the approximation that neither the free charge q nor the potentials V_i have appreciable gradients along the x -axis, the third and fourth terms vanish. The first term gives the four acceleration disturbances noted in the text as A_{11} through A_{14} , which depend on voltage fluctuations δV_i and charge fluctuations δq . The second term gives the four contributions to the spring coupling K noted in the text as K_{s1} through K_{s4} , which depend on fluctuations in the capacitances and their gradients and constitute a spring-like coupling because the resulting forces are proportional to δx (denoted by X_{ps} in the text), which can be viewed as the rms fluctuation in the gap between the PM and the surrounding electrodes along the sensitive (x -) axis.

The following relations, inferred from the above definitions, are helpful in deriving the expressions given in the text for sensor-induced acceleration disturbances. If all C_i are comparable in magnitude and on the order of $C_x \approx 6$ pF ($= \epsilon_0 A_p/d$) for a 2-mm gap, and the gap asymmetry in the x -direction is $\Delta d \equiv d_{x1} - d_{x2}$ with gradients as defined in eq. (A.8), then the gradient of the total capacitance $C \approx 6C_x$ in the x -direction is

$$C' \approx \frac{C_x}{d} \left(\frac{1}{1-\alpha} - \frac{1}{1+\alpha} \right) \approx \frac{C_x}{d^2} \Delta d \equiv \alpha C_x \approx 1.5 \text{ pF/m} \left(\frac{\Delta d}{1 \mu\text{m}} \right) . \quad (\text{A.12})$$

If, in addition, the average of the potentials on opposing faces is the same for all three axes and denoted by $V_{x0} \equiv (V_{x1} + V_{x2})/2$, then the PM potential V_s can be written as the following function of V_{x0} , the stray capacitance to ground C_g , and the voltage to ground V_g :

$$V_s = \left(1 - \frac{C_g}{C} \right) V_{x0} + \frac{C_g}{C} V_g . \quad (\text{A.13})$$

The first contribution to V'_m defined by eq. (A.5) above can be approximated by the following expression:

$$\begin{aligned} (V'_m)_1 &\approx \frac{1}{d} \frac{C_x}{C} [\Delta V_x + 2\alpha(V_{x0} - V_s)] = \frac{1}{d} \frac{C_x}{C} [\Delta V_x + 2\alpha \frac{C_g}{C} (V_{x0} - V_g)] \\ &\approx 0.83 \left(\frac{\Delta V_x}{0.01 \text{ V}} \right) + 7 \times 10^{-4} \left(\frac{\Delta d}{1 \mu\text{m}} \right) \left(\frac{6C_g}{C} \right) \left(\frac{V_{x0} - V_g}{0.1 \text{ V}} \right) \text{ V/m}, \\ \Delta V_x &\equiv V_{x1} - V_{x2}. \end{aligned} \quad (\text{A.14})$$

For a gap asymmetry of a few microns, 4α will be on the order of 0.001. If the average potential V_{x0} across the gaps is no more than about 100 times larger than the potential difference ΔV_x across the gaps, then, since $C_g/C \leq 1$, the second term in $(V'_m)_1$ is negligible. The second contribution takes the form:

$$(V'_m)_2 \approx -\frac{q}{d^2} \frac{C_x}{C^2} \Delta d \approx 1.2 \times 10^{-4} \text{ V/m} \left(\frac{q}{q_0} \right) \left(\frac{\Delta d}{1 \mu\text{m}} \right). \quad (\text{A.15})$$

Finally, assume that the magnitudes of the fluctuations of all of the potentials, δV_i , are identical and equal to the of the average potentials for all three axes *and* for the voltage to ground, all of which will be expressed by δV_{x0} . Note that summations involving capacitance gradients C'_i will involve only $i = x_1, x_2$, while summations involving capacitances C_i will involve all (seven) i . Thus, for example,

$$\sum_i \delta V_i C_i \approx 6C_x \delta V_{x0} + C_g \delta V_g \approx C \delta V_{x0}. \quad (\text{A.16})$$

With these assumptions, the four acceleration disturbances that come from $\delta F_{x,A}$ have the following forms, which reduce to the expressions given in eqs. (30–33) of the text and the numerical values in Table 2.

$$\begin{aligned} A_{11} &= \frac{1}{m_p} \sum_i \delta V_i [C'_i (V_i - V_s) - C_i (V'_m)_1] \\ &\approx \frac{1}{m_p} \frac{C_x}{d} \frac{C_g}{C} (V_{x0} - V_g) \left[\delta(\Delta V_x) - \frac{\Delta d}{d} \delta V_i \right] \\ &\approx 39 \times 10^{-17} \text{ m/s}^2 \sqrt{\text{Hz}} \left(\frac{6C_g}{C} \right) \left(\frac{V_{x0} - V_g}{0.1 \text{ V}} \right) \left(\frac{\delta(\Delta V_x)}{10^{-5} \text{ V}/\sqrt{\text{Hz}}} \right), \end{aligned} \quad (\text{A.17})$$

where it has been assumed that $C_g \approx C/6$. Note that this assumption is critical for preventing this from dominating the entire LISA acceleration disturbance budget. It is *not* the usual condition desired for maximum sensitivity of a capacitive displacement transducer.[7]

$$\begin{aligned} A_{12} &= -\frac{1}{m_p} \sum_i \delta V_i \left[\frac{q}{C} C'_i + C_i (V'_m)_2 \right] \\ &\approx -\frac{1}{m_p} \frac{q}{d} \frac{C_x}{C} \left[\delta(\Delta V_x) - \frac{\Delta d}{d} \delta V_i \right] \\ &\approx -6.4 \times 10^{-17} \text{ m/s}^2 \sqrt{\text{Hz}} \left(\frac{q}{q_0} \right) \left[\left(\frac{\delta(\Delta V_x)}{10^{-5} \text{ V}/\sqrt{\text{Hz}}} \right) - 5 \times 10^{-4} \left(\frac{\Delta d}{1 \mu\text{m}} \right) \left(\frac{\delta V_i}{10^{-5} \text{ V}/\sqrt{\text{Hz}}} \right) \right], \end{aligned} \quad (\text{A.18})$$

where the net free charge on the PM, q has been set to the nominal maximum allowed, $q_0 \equiv 10^{-13} \text{ C}$.

$$\begin{aligned} A_{13} &= -\frac{1}{m_p} (V'_m)_1 \delta q \\ &\approx -\frac{1}{m_p d} \frac{C_x}{C} \left[\Delta V_x + \frac{\Delta d}{d} \frac{C_g}{C} (V_{x0} - V_g) \right] \delta q \\ &\approx -8.3 \times 10^{-17} \text{ m/s}^2 \sqrt{\text{Hz}} \left[\left(\frac{\Delta V_x}{0.01 \text{ V}} \right) + 8.3 \times 10^{-4} \left(\frac{6C_g}{C} \right) \left(\frac{V_{x0} - V_g}{0.1 \text{ V}} \right) \right] \left(\frac{1 \text{ mHz}}{\nu} \right). \end{aligned} \quad (\text{A.19})$$

$$\begin{aligned}
A_{14} &= -\frac{1}{m_p} (V'_m)_2 \delta q \\
&\approx \frac{q}{m_p d} \frac{C_x}{C^2} \frac{\Delta d}{d} \delta q \\
&\approx 1.2 \times 10^{-20} \text{ m/s}^2 \sqrt{\text{Hz}} \left(\frac{q}{q_0} \right) \left(\frac{\Delta d}{1 \mu\text{m}} \right) \left(\frac{1 \text{ mHz}}{\nu} \right), \tag{A.20}
\end{aligned}$$

where the value for δq and its frequency dependence have been taken from eq. (16) of the text.

Similarly, the three classes of contributions to the springlike PM-SC coupling K are found from the expression for $\delta F_{x,K}$ [eqs. (A.11), after division by m_p and δx]. To reduce these to the approximate expressions given in Section 4.3 and Table 3, the following assumptions will be made. First, note that since these contributions all depend on variations of the capacitances or their derivatives to produce a force in the x -direction, none of them will involve capacitances for the other axes, or the capacitance to ground. While forces along the sensitive axis can arise from cross-coupling *via* disturbances along other axes, such effects are not included here. Second, fluctuations in the capacitances C_i along the sensitive axis ($i = x_1, x_2$) are assumed to have the following forms:

$$\delta C_{x1} = -\delta C_{x2} \approx \frac{C_x}{d} \delta x; . \tag{A.21}$$

Third, fluctuations in the capacitance gradients along the x -axis are assumed to be as follows:

$$\delta C'_{x1} = \delta C'_{x2} \approx \frac{C_x}{d^2} \delta x . \tag{A.22}$$

Thus, the three general forms for the sensor-induced contribution to PM-SC coupling K are as follows, with the assumptions above used to reduce them to the estimates given in Section 4.3 above and Table 3.

$$\begin{aligned}
K_{s1} &= \frac{1}{m_p} \left[\frac{1}{2C^2} q^2 \sum_i \frac{\delta C'_i}{\delta x} - (V'_m)_2 \frac{q}{C} \sum_i \frac{\delta C_i}{\delta x} \right] \\
&\approx \frac{1}{m_p C d^2} \left(\frac{C_x}{C} \right) q^2 \\
&\approx 9 \times 10^{-12} / \text{s}^2 \left(\frac{q}{q_0} \right)^2 ; \tag{A.23}
\end{aligned}$$

$$\begin{aligned}
K_{s2} &= \frac{1}{m_p} \frac{-q}{C} \sum_i \frac{\delta C'_i}{\delta x} (V_i - V_s) \\
&\approx -\frac{2}{m_p d^2} \left(\frac{C_x}{C} \right) \left(\frac{C_g}{c} \right) q (V_{x0} - V_g) \\
&\approx 10^{-10} / \text{s}^2 \left(\frac{6C_g}{C} \right) \left(\frac{V_{x0} - V_g}{0.1 \text{ V}} \right) \left(\frac{q}{q_0} \right) ; \tag{A.24}
\end{aligned}$$

$$\begin{aligned}
K_{s3} &= \frac{1}{m_p} \left[(V'_m)_1 \sum_i \frac{\delta C_i}{\delta x} (V_i - V_s) + \frac{1}{2} \sum_i \frac{\delta C'_i}{\delta x} (V_i - V_s)^2 \right] \\
&\approx \frac{1}{m_p} \frac{C_x}{d^2} \left[\frac{C_x}{C} (\Delta V_x)^2 + \left(\frac{C_g}{C} \right)^2 (V_{x0} - V_g)^2 + \frac{1}{4} (\Delta V_x)^2 \right] \\
&\approx 3.4 \times 10^{-10} / \text{s}^2 \left[0.94 \left(\frac{V_{x0} - V_g}{0.1 \text{ V}} \right)^2 + 0.06 \left(\frac{\Delta V_x}{0.01 \text{ V}} \right)^2 \right]. \tag{A.25}
\end{aligned}$$